The Aeronautical Journal (2025), **129**, pp. 1515–1533
doi:10.1017/aer.2024.129

RESEARCH ARTICLE

Distributed cooperative guidance law without numerical singularity with field-of-view angle constraint

Z. Liu[1], S. Li[1,2], L. Ren[1] and D. Ma[1]

[1]High-Tech Institute of Xi'an, Xi'an, China
[2]Department of Automation, Tsinghua University, Beijing, China
Corresponding author: Z. Liu; Email: lzy568811@163.com

Received: 9 February 2024; **Revised:** 1 July 2024; **Accepted:** 28 October 2024

Keywords: distributed; cooperative guidance law; field-of-view constraint; numerical singularity

Abstract

A distributed cooperative guidance law without numerical singularities is proposed for the simultaneous attack a stationary target by multiple vehicles with field-of-view constraints. Firstly, the vehicle engagement motion model is transformed into a multi-agent model. Then, based on the state-constrained consensus protocol, a coordination control law with field-of-view (FOV) constraints is proposed. Finally, the cooperative guidance law has been improved to make it more suitable for practical application. Numerical simulations verified the effectiveness and robustness of the proposed guidance law in the presence of acceleration saturation, communication delays and measurement noise.

Nomenclature

r_i	the distance between the vehicle and target
v_i	the velocity of the vehicle
a_i	the acceleration of the vehicle
u_i	the virtual input of the vehicle
w, B, c	constant in the virtual control law
PNG	proportional navigation guidance
LOS	line of sight
FOV	field-of-view

Greek symbol

σ	leading angle
λ	LOS angle
θ	velocity angle
ψ	yaw angle
ξ	auxiliary variables
ζ	auxiliary variables

1.0 Introduction

With the development and progress of interception and defense systems, it is becoming increasingly difficult for individual vehicles to break through blockades and avoid interception by defense systems [1]. Cooperative attack by multiple vehicles is an effective strategy that can break through defense systems.

© The Author(s), 2024. Published by Cambridge University Press on behalf of Royal Aeronautical Society.

https://doi.org/10.1017/aer.2024.129 Published online by Cambridge University Press

As a result, there has been great progress in cooperative guidance and control technologies in recent years. Existing cooperative guidance research can be classified into two strategies [2]. The first strategy is based on the impact time control guidance (ITCG) law [3], its guidance laws are designed for a single vehicle, and a common desired arrival time for each vehicle is preassigned. The second strategy is to obtain information through communication between the vehicles and use it to generate guidance commands [4].

The ITCG-based simultaneous arrival guidance law has been extensively studied. The ITCG law is proposed in Ref. [3] and applied to multi-missile simultaneous arrival tasks. This has resulted in a plethora of studies investigating the simultaneous arrival problem [5–7]. Although the ITCG-based strategy can achieve simultaneous arrival of multiple vehicles, the preassigned expected arrival time must be carefully selected. Considering the constraints of velocity of the vehicles, an unreasonable expected arrival time may cause the vehicle unable to meet the constraints of simultaneous arrival. The strategy based on information exchange is an effective way to overcome the shortcomings of ITCG-based strategy. A cooperative proportional navigation guidance (CPNG) law is proposed in Ref. [8], which enables a simultaneous arrival by multiple vehicles by designing a time-varying control law for the navigation coefficients. An online optimal cooperative guidance law is designed by applying model predictive control (MPC) techniques in Ref. [9].

In recent years, multi-agent consensus protocols have been widely studied [10–14] and applied to the design of cooperative guidance law for multiple vehicles [15–18]. The remaining flight time is usually used as a coordinate variable and then coordinate variable of multiple vehicles is controlled to converge by designing a consistency protocol, thus enabling simultaneous arrival by multiple vehicles [6, 16]. However, this approach requires the ability to accurately estimate the remaining flight time. A cooperative guidance law with FOV constraints is proposed in Ref. [19], which consists of two phases, namely the arrival time synchronisation phase and proportional navigation phases. In Ref. [20], a guidance law that satisfies both the impact time and impact angle constraints is proposed, however, this guidance law requires the vehicle to have the ability to change its own velocity magnitude. A 3D cooperative guidance law for multiple vehicles based on the event-triggered strategy is proposed in Ref. [17], which can reduce the resource utilisation burden while ensuring the good performance of the guidance law.

Although numerous cooperative guidance law have been proposed up to now, there are still some practical issues that require further attention. First, a significant proportion of cooperative guidance laws do not take into account the vehicle's FOV constraints [21–23]. This can result in target loss of lock during the trajectory adjustment. Second, many cooperative guidance law are afflicted by numerical singularity problem, which could render guidance commands diverge to infinity when the vehicle-target range is close to zero [4, 23]. To circumvent this issue, a two-phase guidance law is frequently employed [19, 24]. However, ensuring the continuity of guidance commands when transitioning between guidance laws remains challenging. Thirdly, the majority of existing cooperative guidance law have not been subjected to rigorous testing to ascertain their effectiveness and robustness in a wide range of scenarios. Nevertheless, these significant issues are seldom discussed in the literature on cooperative guidance due to the highly nonlinear system dynamics involved.

Considering the shortcomings of existing guidance laws, this study proposes a distributed cooperative guidance law with FOV constraints. First, the motion engagement model for vehicle is transformed into a two-integrator model. Then, an arrival time cooperative control law is designed based on the state constraint consensus algorithm. This study's major contributions and innovations are as follows:

(1) A cooperative guidance law considering the FOV constraint is proposed based on the state constraint consensus protocol, which is more feasible and reliable for practical applications.

(2) The proposed guidance law has no numerical singularity, and acceleration is bounded. This means that there is no need to switch the guidance law to avoid numerical singularity problems [19, 24].

https://doi.org/10.1017/aer.2024.129 Published online by Cambridge University Press

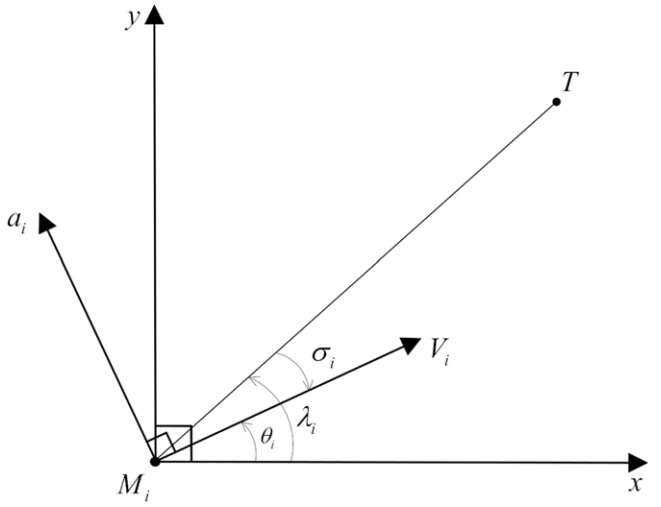


Figure 1. *Two-dimensional vehicle–target engagement geometry.*

(3) The results of the simulation demonstrate that the proposed guidance law is capable of functioning effectively in a variety of guidance scenarios. Furthermore, the guidance law exhibits robust performance even in the presence of communication delays and measurement noise.

The rest of this paper is organised as follows. Section 2 presents the necessary background and problem statement. Section 3 introduces the main results of the study, including the design of a cooperative guidance law. Then, Section 4 presents the numerical simulations and analyses the results. Finally, Section 5 presents the conclusions and prospects.

2.0 Problem statement and preliminaries

2.1 Problem statement

The following assumptions are first introduced:

Assumption 1. *The vehicles and the target are regarded as mass points.*

Assumption 2. *The speed of vehicles is assumed to be constant, and the target is considered to be stationary.*

Considering a scenario in which $N \geqslant 2$ vehicles attack the same static target, Fig. 1 depicts the relative motion between the ith vehicle and the target in the two-dimensional plane, where $M_i - xy$ is a Cartesian inertial reference frame, and M_i and T represent the ith vehicle and target, respectively. The planar kinematics model of vehicle–target engagement can be described as:

$$\dot{r}_i = -v_i \cos \sigma_i \tag{1}$$

$$\dot{\lambda}_i = -\frac{v_i \sin \sigma_i}{r_i} \tag{2}$$

$$\dot{\theta}_i = \frac{a_i}{v_i} \tag{3}$$

$$\theta_i = \lambda_i + \sigma_i \tag{4}$$

https://doi.org/10.1017/aer.2024.129 Published online by Cambridge University Press

where r_i represents the relative distance between the vehicle and the target; v_i represents the speed of the ith vehicle; a_i represents the acceleration of the ith vehicle, which is perpendicular to the speed direction; and $\lambda_i, \theta_i, \sigma_i$ represent the line-of-sight angle, heading angle and leading angle of the ith vehicle, respectively. The positive direction of the angle is counterclockwise.

The purpose of the designed cooperative guidance law is to control N vehicles to reach target T at the same time; that is

$$\left| \frac{r_i}{\dot{r}_i} - \frac{r_j}{\dot{r}_j} \right| \to 0, \forall i \neq j; i, j = 1, 2, \cdots, N \tag{5}$$

Consider that the FOV angle of the vehicle should not exceed its maximum allowable value. With the assumption of a small angle-of-attack [9], the FOV constraint can be approximated as

$$|\sigma_i(t)| < \sigma_{\max} \leq \frac{\pi}{2}, t \geqslant t_0, \forall i = 1, 2, \cdots, N \tag{6}$$

where $\sigma_{\max} > 0$ represents the maximum allowable value of the leading angle of vehicles.

Remark 1. It should be noted that this study considers the isomorphic vehicles; thus, it is assumed that the maximum FOV allowed by each vehicle has the same value; that is, $\sigma_{\max,1} = \sigma_{\max,2} = \cdots = \sigma_{\max,N} = \sigma_{\max}$.

2.2. Preliminaries

2.2.1. Graph theory

The topology of the communication network between the vehicles is described as an undirected weight graph $\mathcal{G}(\mathcal{V}, \mathcal{E})$, where $\mathcal{V} = \{1, \cdots, N\}$ represents the set of nodes, where node i corresponds to the ith vehicle. $\mathcal{E} \subseteq \mathcal{V} \times \mathcal{V}$ represents the set of edges. The neighbourhood set of node i is defined as $\mathcal{N}_i = \{j \in \mathcal{V} | (i, j) \in \mathcal{E}\}$. The adjacency matrix of graph $\mathcal{G}$ is expressed as $A = \left[a_{ij}\right] \in \mathbb{R}^{N \times N}$, and the unordered pair $(i, j) \in \mathcal{E} \Leftrightarrow a_{ij} > 0 \Leftrightarrow$ vehicle i and vehicle j can communicate and exchange information; $a_{ij} = 0 \Leftrightarrow (i, j) \notin \mathcal{E}$. In addition, $a_{ii} = 0, i = 1, 2, \cdots, N$. Finally, the Laplacian matrix of $\mathcal{G}$ is $L = \left[l_{ij}\right] \in \mathbb{R}^{N \times N}$, where $l_{ii} = \sum_{j=1}^{N} a_{ij}$, and $l_{ij} = -a_{ij}, i \neq j$.

To satisfy the simultaneous arrival constraint, the communication topology $\mathcal{G}$ among vehicles needs to satisfy the following assumption.

Assumption 3. *$\mathcal{G}(\mathcal{V}, \mathcal{E})$ is undirected and connected, which means the ith vehicle and the jth vehicle can get information from each other if $\left(v_i, v_j\right) \in \mathcal{E}$, and there is a communication path that involves all vehicles.*

2.2.2 Useful lemmas

Lemma 1. *[25] Consider a second-order multi-agent system with the following dynamical equations:*

$$\dot{\xi}_i = \zeta_i, i = 1, \cdots, N \tag{7}$$

$$\dot{\zeta}_i = u_i, i = 1, \cdots, N \tag{8}$$

with the constraint

$$\zeta_{\min} \leq \zeta_i(t) > \zeta_{\max}, t \geq t_0, i = 1, 2, \cdots, N, \tag{9}$$

where $\xi_i, \zeta_i \in \mathbb{R}^m$ denote the state of the ith agent; $u_i \in \mathbb{R}^m$ denotes the input of the ith agent; and $\zeta_{\min} = \left[\zeta_{\min}^1, \cdots, \zeta_{\min}^m\right]^T, \zeta_{\max} = \left[\zeta_{\max}^1, \cdots, \zeta_{\max}^m\right]^T$ is a constant value.

https://doi.org/10.1017/aer.2024.129 Published online by Cambridge University Press

If the following conditions are satisfied,

(1) the communication topology $\mathcal{G}$ among agents is undirected and connected;

(2) (2) $\zeta_i(t_0) \in [\zeta_{\min}, \zeta_{\max}], i = 1, 2, \cdots, N$; and the consensus protocol is designed as

$$u_i = -K(\zeta_i - \zeta_{ir}) \tag{10}$$

$$\zeta_{ir} = w + Bf\left(K_e \sum_{j \in \mathcal{N}_i} a_{ij}(\xi_i - \xi_j) + c\right) \tag{11}$$

where $K, K_e \in \mathbb{R}^{m \times m}$ are a positive definite diagonal matrix; a_{ij} is the element of the adjacency matrix A; and $f(\cdot)$ is a continuous function that has the following properties:

P1: $f(\cdot)$ is a strictly increasing function;

P2: $f(0) = 0$;

P3: $\lim_{x \to +\infty} f(x) = 1$;

P4: $\lim_{x \to -\infty} f(x) = -1$.

w, B, and C are defined as follows:

$$w = \frac{\zeta_{\min} + \zeta_{\max}}{2} \tag{12}$$

$$B = \frac{1}{2}\mathrm{diag}\left\{\zeta^1_{\max} - \zeta^1_{\min}, \cdots, \zeta^m_{\max} - \zeta^m_{\min}\right\} \tag{13}$$

$$c = f^{-1}\left(B^{-1}(w - \zeta_d)\right) \tag{14}$$

where $f^{-1}(\cdot)$ denotes an inverse function of $f(\cdot)$, and ζ_d denotes the reference value of $\zeta_i, i = 1, 2, \cdots, N$.

Then, the multi-agent system Equations (7) and (8) will reach consensus without violating the constraint Equation (9); that is, $\xi_i \to \xi_j$ and $\zeta_i \to \zeta_d$ asymptotically as $t \to \infty$.

Remark 2. The four properties of function $f(\cdot)$ mentioned in Lemma 1 are actually not strict. For example, functions such as $tanh\, x = \frac{e^x - e^{-x}}{e^x + e^{-x}}$, $\frac{2}{\pi}\, arctan\, x$ all have these properties.

3.0 Cooperative guidance law design

3.1 Engagement model transformation

Let $y_{v,i} = r_i \sin\sigma_i$ denote the component of r_i in the direction perpendicular to the velocity of the ith vehicle. When σ_i is small, we take the second derivative of $y_{v,i}$ and substitute $\sin\sigma_i \approx \sigma_i$, $\cos\sigma_i \approx 1$. Then,

$$\ddot{r}_i\sigma_i + 2\dot{r}_i\dot{\sigma}_i + r_i\ddot{\sigma}_i = \ddot{y}_{v,i} = a_i \tag{15}$$

Therefore, we design

$$a_i = \sigma_i u_i + 2\dot{r}_i\dot{\sigma}_i + r_i\ddot{\sigma}_i \tag{16}$$

where u_i is a virtual control signal of vehicle i. Substituting Equation (16) into (15) yields

$$\ddot{r}_i = u_i \tag{17}$$

Thus, the nonlinear model has been transformed into a double-integrator model. In addition, substituting Equations (1), (3) and (4) into Equation (16), we have

$$a_i = \sigma_i u_i + \frac{2}{3}v\dot{\lambda}_i + \frac{1}{3}r_i\ddot{\sigma}_i \tag{18}$$

Remark 3. It should be noted that the Equation (15) was derived with the assumption of a small leading angle. However, this is not a hard constraint that must be strictly satisfied for the subsequent proposed

https://doi.org/10.1017/aer.2024.129 Published online by Cambridge University Press

guidance law. The reason is that the small leading angle assumption was not considered in the subsequent proof of the convergence of the guidance law.

To convert the FOV constraints of the vehicles into the state constraint of the agents, two auxiliary variables are introduced; that is,

$$\xi_i = \frac{r_i}{v_i} \tag{19}$$

$$\zeta_i = \frac{\dot{r}_i}{v_i} \tag{20}$$

Based on Equation (17), we can obtain

$$\dot{\xi}_i = \zeta_i \tag{21}$$

$$\dot{\zeta}_i = \frac{u_i}{v_i} \tag{22}$$

Then, the simultaneous arrival constraint Equation (5) is equivalent to

$$\left|\xi_i - \xi_j\right| \to 0, \left|\zeta_i - \zeta_j\right| \to 0, \forall i \neq j; i, j = 1, 2, \cdots, N \tag{23}$$

Furthermore, note that $\zeta_i = -\cos\sigma_i$; then, the constraint Equation (6) can be converted to

$$-1 = \zeta_{\min} \leq \zeta_i \leq \zeta_{\max} = -\cos\sigma_{\max} \tag{24}$$

Here, we used the fact that $0 \leq |\sigma_i| \leq \sigma_{\max} < \frac{\pi}{2}$. As a result, the engagement model is transformed into a multi-agent system, so that we can achieve simultaneous arrivals by controlling the states of multi-agent reach consensus. At the same time, the FOV constraints of the vehicles are transformed into state constraints of the agents.

3.2 Coordinated control of arrival time

Based on Equations (21) and (22) and Lemma 1, u_i is designed as

$$u_i = -Kv_i\left[\zeta_i - w + B\tanh\left(K_e\sum_{j=1}^{n} a_{ij}\left(\xi_i - \xi_j\right) + c\right)\right] \tag{25}$$

where K and K_e are parameters that need to be designed; v_i is the velocity of the ith vehicle; ξ_i and ζ_i are defined in Equations (19) and (20), respectively; and a_{ij} is an element of the adjacency matrix A corresponding to the communication topology of vehicles. w, B and c are defined as follows:

$$w = \frac{-\cos\sigma_{\max} - 1}{2}, \tag{26}$$

$$B = \frac{-\cos\sigma_{\max} + 1}{2}, \tag{27}$$

$$c = \tanh^{-1}\left(B^{-1}\left(w + \cos\sigma_d\right)\right). \tag{28}$$

where σ_d is the expected value of σ_i.

Remark 4. From the point of view of the vehicle successfully reaching the target, σ_d should be set to 0. On the other hand, it should be note that $c \to +\infty$ when $\sigma_d = 0$. But the numerical singularity problem still would not occur, because $u_i = -Kv_i\left(\zeta_i - w + B\right)$ when $c \to +\infty$, and in practical, we take c to be large enough to ensure sufficient accuracy for convenience of calculation.

Let $\zeta_{ir} = w - B\tanh\left(K_e\sum_{j=1}^{n} a_{ij}\left(\xi_i - \xi_j\right) + c\right)$; then, Equation (25) could be rewritten as

$$u_i = -Kv_i\left(\zeta_i - \zeta_{ir}\right). \tag{29}$$

https://doi.org/10.1017/aer.2024.129 Published online by Cambridge University Press

Note that $\zeta_{ir} \in [\zeta_{\min}, \zeta_{\max}]$, then $|u_i| \leq Kv_i(\zeta_{\max} - \zeta_{\min})$. Since $a_i = \sigma_i u_i + 2\dot{r}_i\dot{\sigma}_i + r_i\ddot{\sigma}_i$, it is obvious that the second term and the third term are bounded; thus, a_i is also bounded.

3.3 Modified cooperative guidance law

Although a cooperative guidance law that takes into account the FOV constraint can be obtained by substituting Equation (25) into (18). However, note that there is a high-order term that includes $\ddot{\sigma}_i$ in Equation (18), and it is difficult to obtain an accurate value of Equation (18), either from actual measurements or from numerical simulations.

To inherit the nonnumerical singularity of Equation (18) and avoid its disadvantage, we modify it and propose a cooperative guidance law considering the FOV constraint as follows:

$$\begin{aligned} a_i &= a_i^{PNG} + a_i^{BT} \\ &= N_p v_i \dot{\lambda}_i - K v_i \sigma_i \left[\zeta_i - w + B\tanh\left(K_e \sum_{j=1}^{n} a_{ij}\left(\xi_i - \xi_j\right) + c \right) \right], \end{aligned} \tag{30}$$

where $a_i^{PNG} = N_p v_i \dot{\lambda}_i$ is the PNG term; here, $N_p = 3$ is the navigation constant. $a_i^{BT} = \sigma_i u_i = -Kv_i\sigma_i\left[\zeta_i - w + B\tanh\left(K_e\sum_{j=1}^{n} a_{ij}\left(\xi_i - \xi_j\right) + c\right)\right]$ is the arrival time coordination term, where the variables have the same definition as in Equation (25).

Compared with Equations (18), (30) has two improvements. First, the navigation constant has been modified to $N_p = 3$. This is because the cooperative guidance law will become a PNG law when the arrival time of each vehicle is synchronised, and it has been shown that $N_p = 3$ can lead to stable and efficient guidance performance in practice [19, 24]. Second, the term $r_i\ddot{\sigma}_i/3$ is discarded in Equation (30). The reason is that it is difficult to obtain an accurate value of $\ddot{\sigma}_i$ in both practical application and numerical simulation. In addition, even if this term has been discarded, it will not affect guidance performance, which will be shown in the following numerical simulations.

Theorem 1. *Under the conditions that assumptions 1, 2, 3 hold, the guidance law Equation (30) will control the simultaneous arrival of all vehicles and will always not violate the FOV constraints.*

Proof. According to Equations (3), (4), we have that

$$\dot{\sigma}_i = \frac{a_i}{v_i} - \dot{\lambda}_i \tag{31}$$

Substituting Equations (29), (30) into Equation (31) yields

$$\begin{aligned} \dot{\sigma}_i &= \left(N_p - 1\right)\dot{\lambda}_i - K\sigma_i\left(\zeta_i - \zeta_{ir}\right) \\ &= -K\sigma_i\left(\zeta_i - \zeta_{ir}\right) - \left(N_p - 1\right)\frac{v_i \sin\sigma_i}{r_i} \end{aligned} \tag{32}$$

Note that $\zeta_i = -\cos\sigma_i$ and $-1 \leq \zeta_{ir} \leq -\cos\sigma_{\max}$, so we have that

$$\zeta_i + \cos\sigma_{\max} \leq \left(\zeta_i - \zeta_{ir}\right) \leq \zeta_i + 1 \tag{33}$$

when $\sigma_i = \pm\sigma_{\max}$, it can be obtained that

$$0 \leq \left(\zeta_i - \zeta_{ir}\right) \leq -\cos\sigma_{\max} + 1 \tag{34}$$

Therefore, we can have that

$$\dot{\sigma}_i|_{\sigma_i = \sigma_{\max}} = -K\sigma_{\max}\left(\zeta_i - \zeta_{ir}\right) - \left(N_p - 1\right)\frac{v_i \sin\sigma_{\max}}{r_i} < 0 \tag{35}$$

and

$$\dot{\sigma}_i|_{\sigma_i = -\sigma_{\max}} = K\sigma_{\max}\left(\zeta_i - \zeta_{ir}\right) + \left(N_p - 1\right)\frac{v_i \sin\sigma_{\max}}{r_i} > 0 \tag{36}$$

https://doi.org/10.1017/aer.2024.129 Published online by Cambridge University Press

So, we can obtain that the $[0, \sigma_{\max})$ is a positive invariant set of $|\sigma|$, which also means that the field-of-view constraints of vehicles Equation (6) are never violated.

Then, substituting Equation (32) into Equation (22) yields

$$\dot{\zeta}_i = -\Phi_i\left(\zeta_i - \zeta_{ir}\right) - \left(N_p - 1\right)\frac{v_i \sin^2\sigma_i}{r_i} \tag{37}$$

where $\Phi_i = K\sigma_i \sin\sigma_i \geqslant 0$. It can be seen that the $\dot{\zeta}_i$ has two parts, then we consider the effect of these two terms on ζ_i and their convergence separately.

The first term is $-\Phi_i\left(\zeta_i - \zeta_{ir}\right)$, because $\Phi_i \geqslant 0$ always holds, it is obvious that the first term would control the ζ_i converge to ζ_{ir} gradually. Then based on the Lemma 1, we can obtain that the first term $-\Phi_i\left(\zeta_i - \zeta_{ir}\right)$ would control the system Equations (21), (22) reach to consensus, and we can have that $\zeta_i \to \zeta_d$ as $t \to \infty$, that is $\sigma_i \to \sigma_d = 0$. The second term is $-\left(N_p - 1\right) v_i \sin^2\sigma_i / r_i$, because $-\left(N_p - 1\right) v_i \sin^2\sigma_i / r_i \leq 0$ always holds, this will control the ζ_i keep decreasing until $\zeta_i = -1$, that is $\sigma_i = 0$.

Finally, according to the superposition principle, we could obtain that the vehicles will arrive at the target simultaneously and will always not violate the FOV constraints.

Remark 5. It can be observed that the small leading angle assumption was not used in the process of theorem proving, despite its consideration during the design of the guidance law. This implies that the satisfaction or otherwise of the small angle assumption does not affect the convergence of the proposed guidance law. In addition, even if the leading angles do not satisfy the small angle assumption, there is no significant impact on the performance of the guidance law, as will be demonstrated by the subsequent numerical simulations.

Remark 6. The arrival time coordinated control term of the proposed guidance law is $\sigma_i u_i$. This means that when σ_i is small, even if the arrival time synchronisation error is large, a_i^{BT} is still small. However, $\sigma_i \to 0$ means the velocity of the vehicle is in line with the line of sight, which helps the vehicle reach the target. This means the guidance law proposed in this study gives the highest priority to reaching the target, while arrival time synchronisation is the secondary priority. After all, successfully reaching the target is the most important task of guidance.

3.4 Extension of the three-dimensional case

Figure 2 depicts the geometry of the relative motion of the *i*th vehicle–target in 3D space, where $M_i - X_t Y_t Z_t$, $M_i - X_m Y_m Z_m$ denote the inertial reference frame and the velocity frame, respectively.

First, the model of vehicle–target engagement motion in 3D space [26] is given as follows:

$$\dot{r}_i = -v_i \cos\theta_{mi} \cos\psi_{mi}, \tag{38}$$

$$\dot{\theta}_{Li} = \frac{-v_i \sin\theta_{mi}}{r_i}, \tag{39}$$

$$\dot{\psi}_{Li} = \frac{-v_i \cos\theta_{mi} \sin\psi_{mi}}{r_i \cos\theta_{Li}}, \tag{40}$$

$$\dot{\theta}_{mi} = \frac{a_{zi}}{v_i} - \dot{\psi}_{Li} \sin\psi_{Li} \sin\psi_{mi} - \dot{\theta}_{Li} \cos\psi_{mi}, \tag{41}$$

$$\dot{\psi}_{mi} = \frac{a_{yi}}{v_i \cos\theta_{mi}} + \dot{\psi}_{Li} \sin\psi_{Li} \cos\psi_{mi} \tan\theta_{mi} - \dot{\theta}_{Li} \sin\psi_{mi} \tan\theta_{mi} - \dot{\psi}_{Li} \cos\theta_{Li}, \tag{42}$$

where r_i is the relative distance between the *i*th vehicle and the target; v_i denotes the velocity of the *i*th vehicle; and a_{yi}, a_{zi} denote the acceleration of the *i*th vehicle on pitch channel and yaw channel, respectively. The definitions of $\theta_{Li}, \psi_{Li}, \theta_{mi}, \psi_{mi}$ are shown in Fig. 2; counterclockwise is positive. In

https://doi.org/10.1017/aer.2024.129 Published online by Cambridge University Press

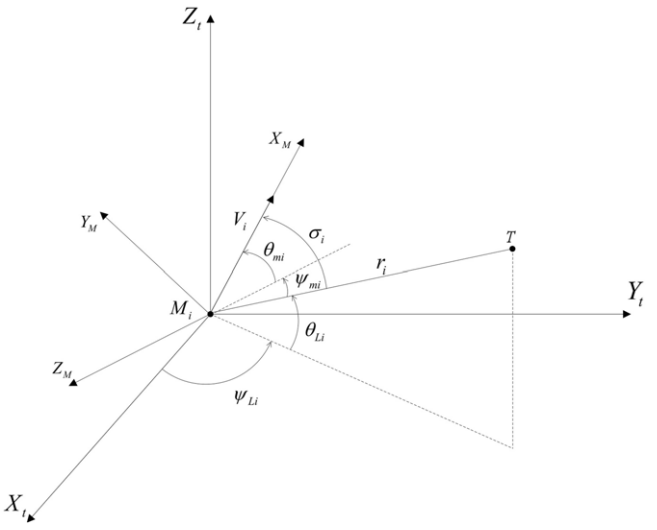


Figure 2. *Three-dimensional vehicle–target engagement geometry.*

addition, the leading angle σ_i of the ith vehicle in 3D space is defined as

$$\sigma_i = \arccos(\cos\theta_{mi}\cos\psi_{mi})\,. \tag{43}$$

The vehicle–target engagement plane is defined as a plane determined by the velocity and line-of-sight direction of the vehicle. In fact, the vehicle–target model in the 3D case can be regarded as a 2D model in the vehicle–target engagement plane; that is, $\vec{a}_i$, $\vec{v}_i$, and $\vec{r}_i$ are in the same plane. Hence, to extend Equation (30) to the 3D case, we could simply rewrite it in vector form:

$$\vec{a}_i = \vec{a}_i^{PNG} + \vec{a}_i^{BT}, \tag{44}$$

where $\vec{a}_i^{PNG}$ is the PNG term, and $\vec{a}_i^{BT}$ is the arrival time synchronisation term. Let a_i^{PNG}, a_i^{BT} denote the module of $\vec{a}_i^{PNG}$, $\vec{a}_i^{BT}$, respectively. Then, according to Equation (30), we have

$$a_i^{PNG} = -\frac{NV_i\sin\sigma_i}{r_i}, \tag{45}$$

$$_i^{BT} = -KV_i\sigma_i\left[\zeta_i - w + B\tanh\left(K_e\sum_{j=1}^{n}a_{ij}\left(\xi_i-\xi_j\right)+c\right)\right]. \tag{46}$$

Let $a_{y,i}^{PNG}$, $a_{z,i}^{PNG}$ denote the components of $\vec{a}_i^{PNG}$ on the M_iX_m, M_iY_m axes, respectively. Following Ref. [26], $a_{y,i}^{PNG}$, $a_{z,i}^{PNG}$ are expressed as follows:

$$a_{y,i}^{PNG} = -\frac{NV_i^2}{r_i}\sin\psi_{mi}, \tag{47}$$

$$a_{z,i}^{PNG} = -\frac{NV_i^2}{r_i}\sin\theta_{mi}\cos\psi_{mi}. \tag{48}$$

We can easily get that $\vec{a}_i^{PNG}$ is coplanar with $\vec{v}_i$ and $\vec{r}_i$ from Equations (47) and (48). Then, we need to determine $a_{y,i}^{BT}$, $a_{z,i}^{BT}$, which are the components of $\vec{a}_i^{BT}$ on the M_iX_m, M_iY_m axes, respectively. Consider that $\vec{a}_i$ must be coplanar with $\vec{v}_i$ and $\vec{r}_i$, which means $\vec{a}_i^{BT}$ and $\vec{a}_i^{PNG}$ are collinear. Therefore, we can get

$$\frac{a_{y,i}^{BT}}{a_{z,i}^{BT}} = \frac{a_{y,i}^{PNG}}{a_{z,i}^{PNG}} = \frac{\tan\psi_{mi}}{\sin\theta_{mi}}. \tag{49}$$

https://doi.org/10.1017/aer.2024.129 Published online by Cambridge University Press

Table 1. *Initial states in the 2D scenario*

State	Vehicle 1	Vehicle 2	Vehicle 3	Target
Position (m)	$[-11,000, -2,000]$	$[0, -12,000]$	$[12,000, -4,000]$	$[0, -2,000]$
v, (m/s)	310	320	330	0
θ, (deg)	30	45	135	–

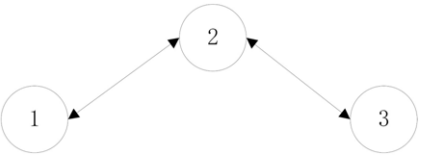


Figure 3. *Network topology of vehicles in a 2D scenario.*

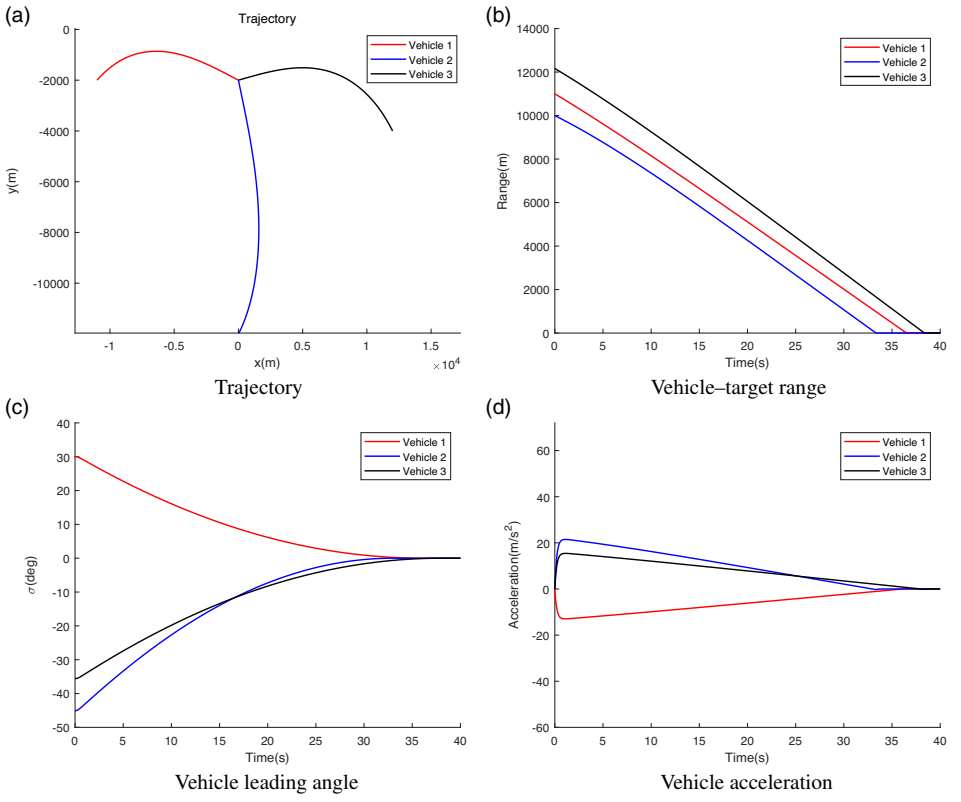


Figure 4. *Guidance results from PNG.*

https://doi.org/10.1017/aer.2024.129 Published online by Cambridge University Press

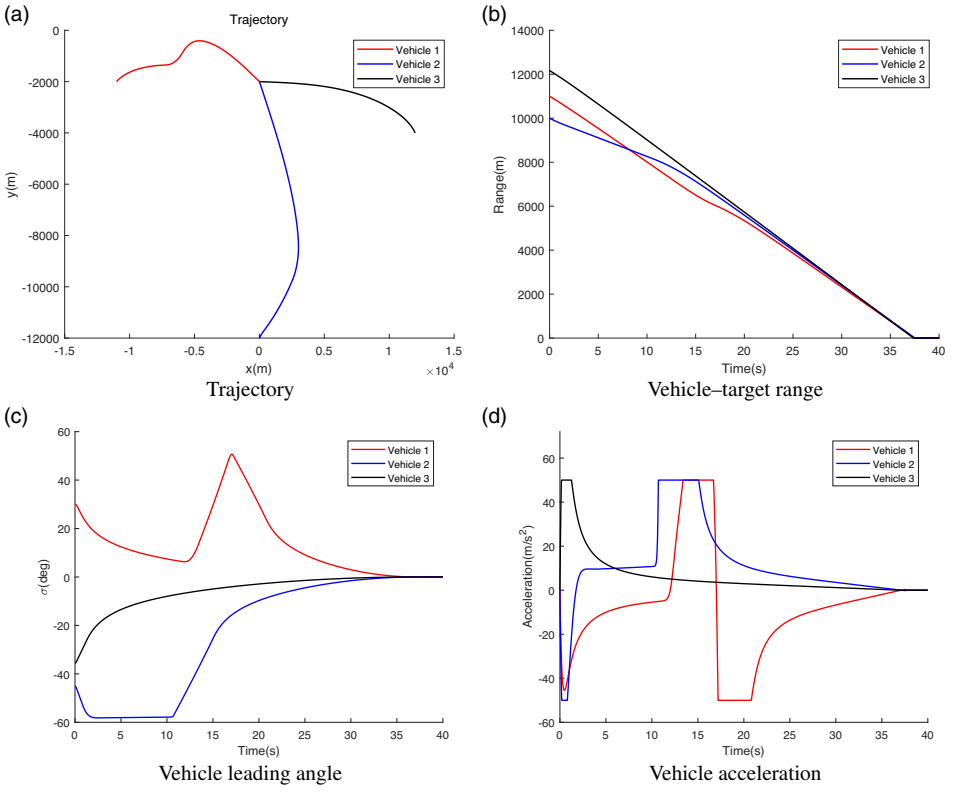


Figure 5. *Guidance results from the proposed guidance law.*

In addition, $a_{y,i}^{BT}, a_{z,i}^{BT}$ also need to satisfy the following constraints:

$$\sqrt{a_{y,i}^{BT2} + a_{z,i}^{BT2}} = a_i^{BT}. \tag{50}$$

Then, combining Equations (49) and (50), we can get

$$a_{y,i}^{BT} = \frac{\sin \psi_{mi}}{\sin \sigma_i} a_i^{BT}, \tag{51}$$

$$a_{z,i}^{BT} = \frac{\sin \theta_{mi} \cos \psi_{mi}}{\sin \sigma_i} a_i^{BT}. \tag{52}$$

Then, combining Equations (44), (47), (48), (51) and (52), the cooperative guidance law with FOV constraints in the 3D case is obtained; that is,

$$a_{y,i} = -\frac{NV_i^2}{r_i} \sin \psi_{mi} + \frac{\sin \psi_{mi}}{\sin \sigma_i} a_i^{BT}, \tag{53}$$

$$a_{z,i} = -\frac{NV_i^2}{r_i} \sin \theta_{mi} \cos \psi_{mi} + \frac{\sin \theta_{mi} \cos \psi_{mi}}{\sin \sigma_i} a_i^{BT}, \tag{54}$$

where $a_{y,i}, a_{z,i}$ denote the components of a_i on the M_iX_m, M_iY_m axes, respectively. a_i^{BT} is defined in Equation (46).

https://doi.org/10.1017/aer.2024.129 Published online by Cambridge University Press

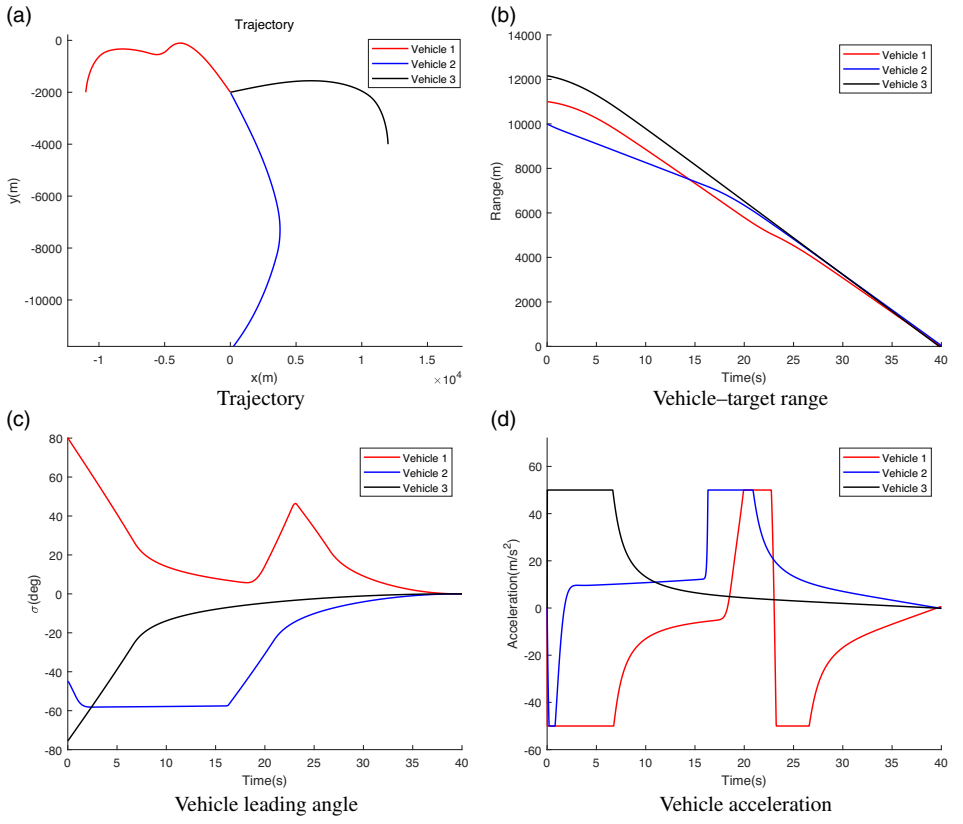


Figure 6. *Guidance results with* $\sigma_1\ (t_0)$, $\sigma_3\ (t_0)$ *violated constraints.*

Note that $\sin\sigma_i$ appears in the denominator of the expression for $a_{y,i}^{BT}$, $a_{z,i}^{BT}$, and it follows that $\sin\sigma_i = 0$ when $\sigma_i = 0$ or $\sigma_i = \pi$. However, there are still no numerical singularities in the proposed cooperative guidance law in the 3D case.

(1) $\sigma_i = 0$. Then, $\sin\sigma_i$ could be canceled out by σ_i in a_i^{BT}, because it is always true that $\lim\limits_{\sigma_i \to 0} \frac{\sigma_i}{\sin\sigma_i} = 1$.

(2) $\sigma_i = \pi$. This means $\vec{v}_i$ is opposite to $\vec{r}_i$; that is, the vehicle is moving away from the target. Such an extreme situation is unlikely to occur in practice.

3.5 Parameter selection

The proposed cooperative guidance law mainly involves three parameters: K, K_e and σ_d. The value of K determines the importance of the time coordination term a_i^{BT} relative to the PNG term a_i^{PNG}. From the standpoint of improving arrival time synchronisation error convergence speed, we should have K be as large as possible. However, a too-large K value might result in the vehicle not reaching the target accurately. On the other hand, K should not be too small since it will lead to the guidance law being very close to the PNG law. In addition, K_e, σ_d should be selected carefully. A larger K_e means it is more sensitive to arrival time synchronisation error. However, this might lead to a vibration of the vehicle state, and a smaller K_e means the arrival time synchronisation error will be put in a less-important position. In general, σ_d should be chosen as 0, but this will lead to $c \to \infty$. Furthermore, the arrival time synchronisation error convergence speed will be slowed down when σ_d is too close to the constraint boundary. Even so, we still need to have σ_d be as close to 0 as possible to ensure the vehicle can reach the target.

https://doi.org/10.1017/aer.2024.129 Published online by Cambridge University Press

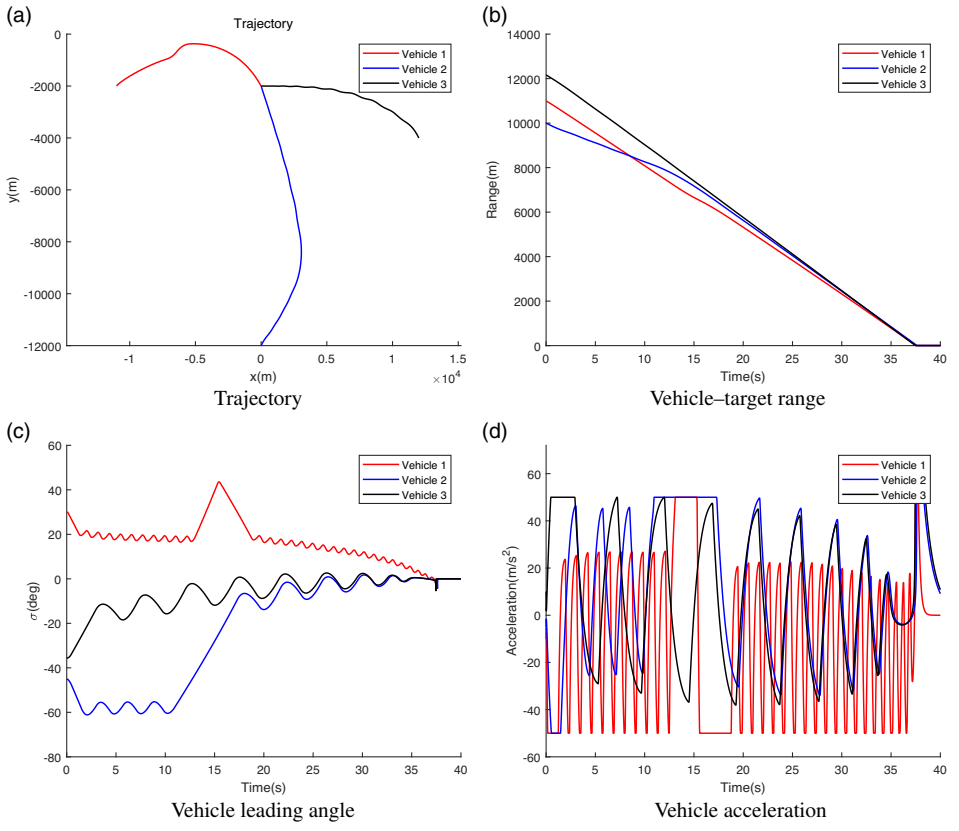


Figure 7. *Guidance results from Equation (18).*

In conclusion, the above analysis provides a reference for determining the the values of K, K_e, σ_d. But for different scenarios, their parameter values still need to be adjusted slightly.

4.0 Numerical simulation

Here, we perform several examples of numerical simulations to demonstrate the effectiveness of the proposed guidance law. The parameters involved in the proposed guidance law are chosen as follows:

$$K = 2, \quad K_e = 8, \quad \sigma_d = 0.001 \ rad. \tag{55}$$

Although the performance of different simulation scenarios can be improved by carefully tuning the value of parameters, in order to verify the robustness of the proposed guidance law, the same parameter values are used in different simulation examples.

In addition, all simulation examples use the following settings. The simulation step size is fixed as 0.02 s. The vehicle will stop the simulation when the distance between the vehicle and the target is less than 0.5 m; otherwise, it is assumed that it has not successfully reached the target. The FOV limit and the maximum acceleration magnitude of the vehicle are set to $\sigma_{\max} = \pi/3$ and $a_{\max} = 50\ \mathrm{m/s^2}$, respectively. The autopilot of the vehicle is considered a first-order lag system; that is,

$$\frac{a_m}{a_{mc}} = \frac{1}{Ts+1}, \tag{56}$$

https://doi.org/10.1017/aer.2024.129 Published online by Cambridge University Press

Table 2. *Initial states in the 3D scenario*

States	Vehicle 1	Vehicle 2	Vehicle 3	Vehicle 4
r (km)	18	16	14	12
v (m/s)	350	340	320	300
θ_L (deg)	-65	-50	-25	-5
ψ_L (deg)	15	25	45	65
θ_m (deg)	-35	-15	25	35
ψ_m (deg)	-45	-25	25	45

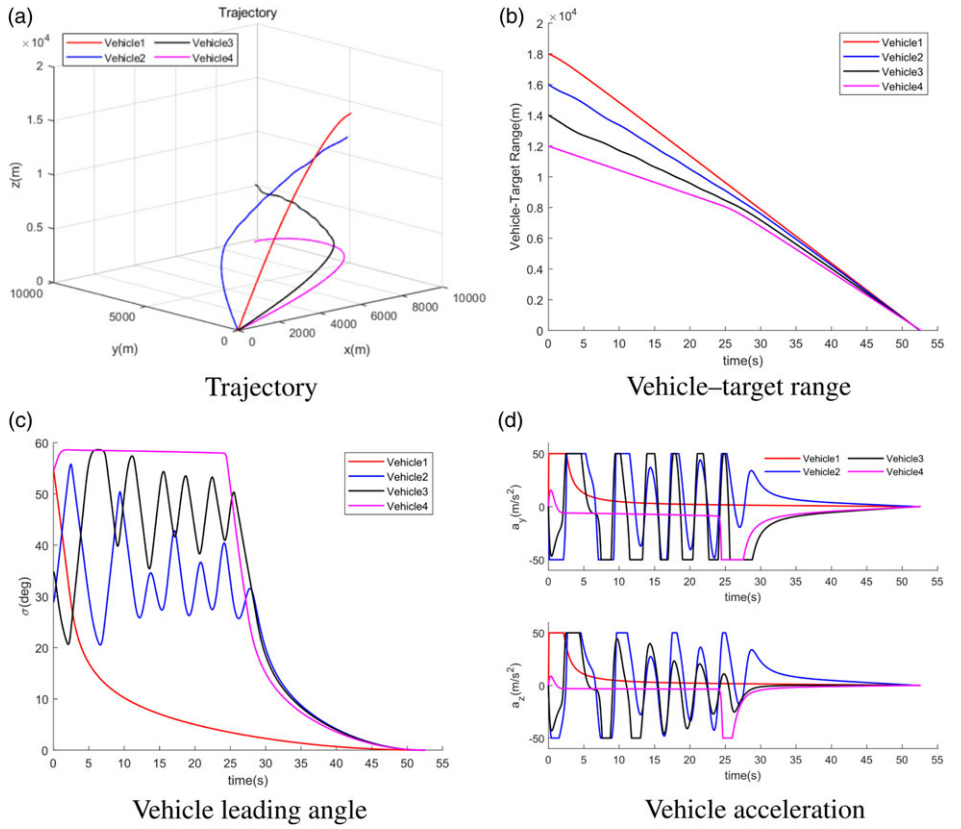


Figure 8. *Guidance results from the proposed 3D guidance law.*

where a_m, a_{mc} denote the real value and commanded value of acceleration, respectively. T is chosen as 0.2s in the simulation.

4.1 Two-dimensional simulation scenarios

Consider a scenario in which three vehicles cooperatively attack one stationary target in the plane. The initial states of the vehicles and the target are listed in Table 1. Figure 3 shows the communication

https://doi.org/10.1017/aer.2024.129 Published online by Cambridge University Press

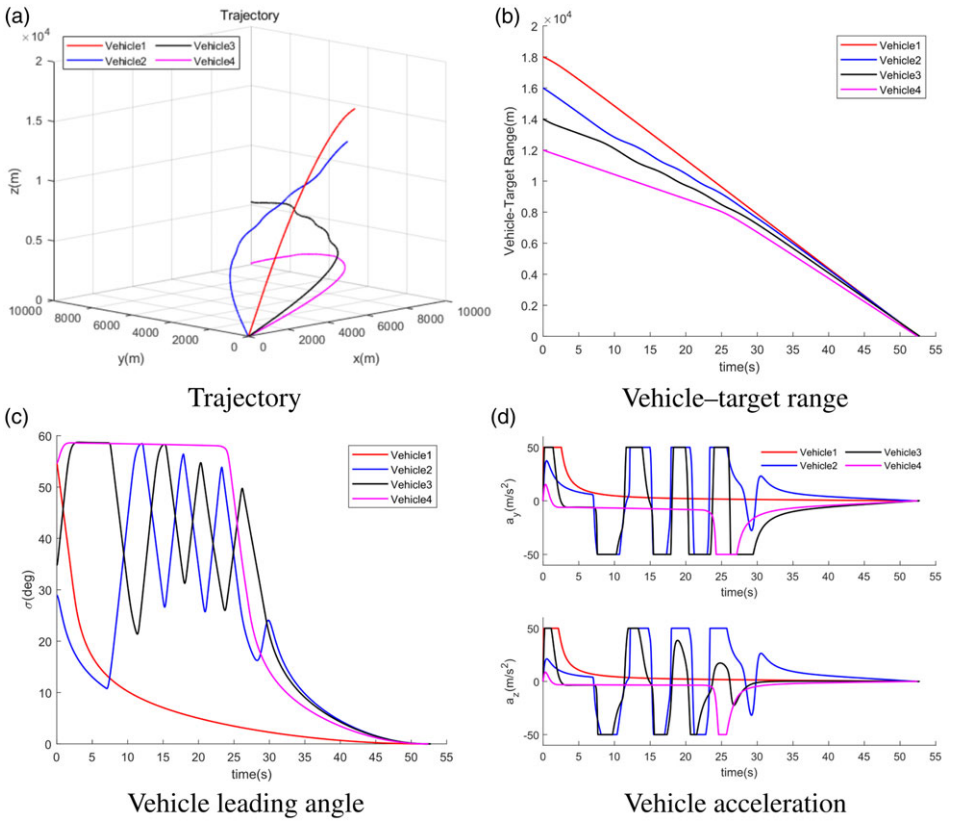


Figure 9. *Guidance results with different network topology.*

topology of the vehicles, and the corresponding adjacency matrix is given in the following:

$$A = \begin{bmatrix} 0 & 1 & 0 \\ 1 & 0 & 1 \\ 0 & 1 & 0 \end{bmatrix}. \tag{57}$$

The PNG law and the proposed guidance law were simulated separately to illustrate the effectiveness of the proposed guidance law. As shown in Fig. 4, the arrival time error for the three vehicles is approximately 5 seconds. However, we can see in Fig. 5 that in this study's proposed guidance law, three vehicles reaching the target simultaneously, and the FOV constraints are never violated.

To facilitate comparison, it is necessary to revisit the guidelines proposed in Ref. [19]. The guidance law proposed in Ref. [19] is as follows:

$$a_i = -\frac{v_i^2 \sin \sigma_i}{r_i} + \frac{u_i}{\sin \sigma_i}, \tag{58}$$

where u_i denotes a virtual input for synchronising the arrival time of vehicles. Note that a_i will diverge to infinity when $\sigma_i \to 0$; thus, the guidance law has to switch to PNG at the final stage.

According to Lemma 1, our proposed guidance law requires the initial leading angle of each vehicle to meet the FOV constraints. The extreme case in which the initial leading angle of some vehicles violates the constraints is considered, where $\theta_1\ (t_0) = 80\ \text{deg}, \theta_3\ (t_0) = 95\ \text{deg}$. We assume, however, that vehicle 1 and vehicle 3 can obtain the position of the target by communicating with vehicle 2 at the start of the guidance. The simulation results are shown in Fig. 6. We can see that although the FOV constraints

https://doi.org/10.1017/aer.2024.129 Published online by Cambridge University Press

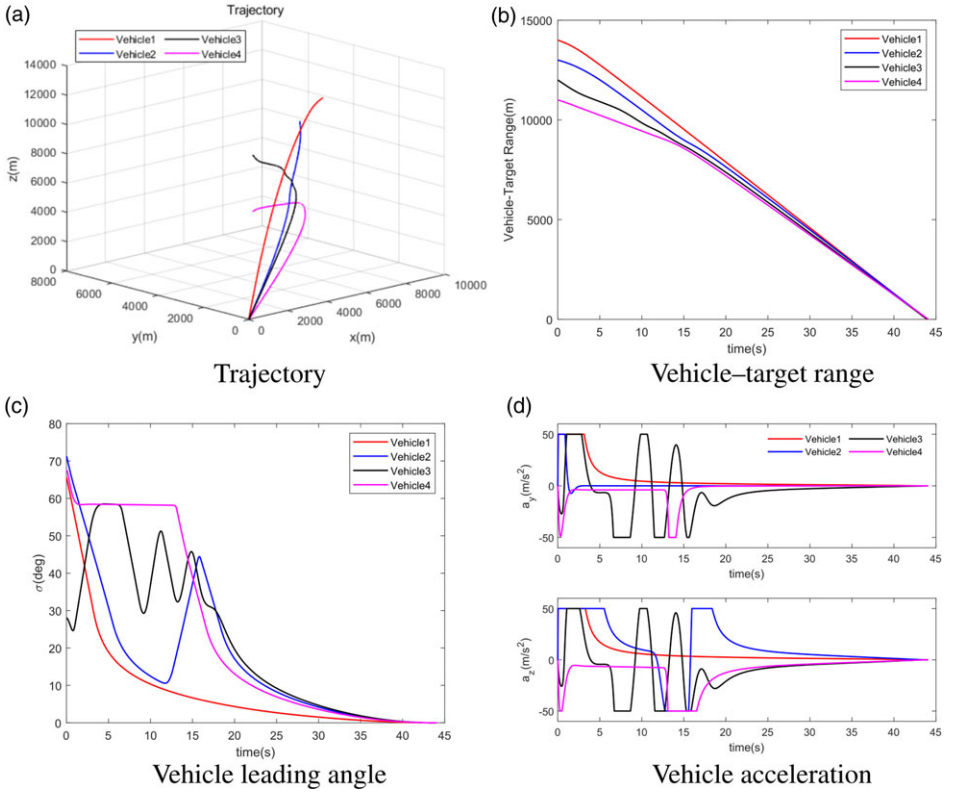


Figure 10. *Guidance results with* $\sigma_1(t_0)$, $\sigma_2(t_0)$, $\sigma_4(t_0)$ *violated constraints.*

are violated at the beginning of the guidance, the guidance law does not collapse, and it still works. Furthermore, σ_1 and σ_3 rapidly converge to the constraint region and are maintained until reaching the target.

It should be noted that the term $r_i\ddot{\sigma}_i/3$ was discarded. To evaluate its effect, the simulation results from Equation (18) are shown in Fig. 7. Note that $\ddot{\sigma}_i = \dot{a}_i/v_i - \ddot{\lambda}_i$. To avoid an algebraic loop in the simulation process, signal delay and difference are used to compute this term. This approach inevitably introduces numerical error, but it at least shows us the effect of the third term. As shown in Fig. 7, although Equation (18) can perform the guidance task effectively, the leading angle and acceleration of the vehicles show severe oscillation. This is due to the fact although $\ddot{\sigma}_i$ is relatively small, r_i is very large, which results in the third term dominating the Equation (18). As the sign of $\ddot{\sigma}_i$ undergoes a series of changes, the resulting acceleration a_i oscillates, which in turn causes the value of $\dot{\sigma}_i$ to oscillate, this is because $\dot{\sigma}_i = a_i/v_i - \dot{\lambda}_i$. Again, this cause the sign of $\ddot{\sigma}_i$ to keep changing. This process will continue until the values of σ_i, $\dot{\sigma}_i$ and r_i gradually approach 0.

4.2 Three-dimensional simulation scenarios

To validate the effectiveness of the proposed guidance law for the 3D case, the following simulations are performed. Considering a scenario with four vehicles and one stationary target whose location is (0 m, 0 m, 0 m). The initial states of the vehicles are listed in Table 2. The adjacency matrix corresponding to the communication topology of the vehicles is as follows:

https://doi.org/10.1017/aer.2024.129 Published online by Cambridge University Press

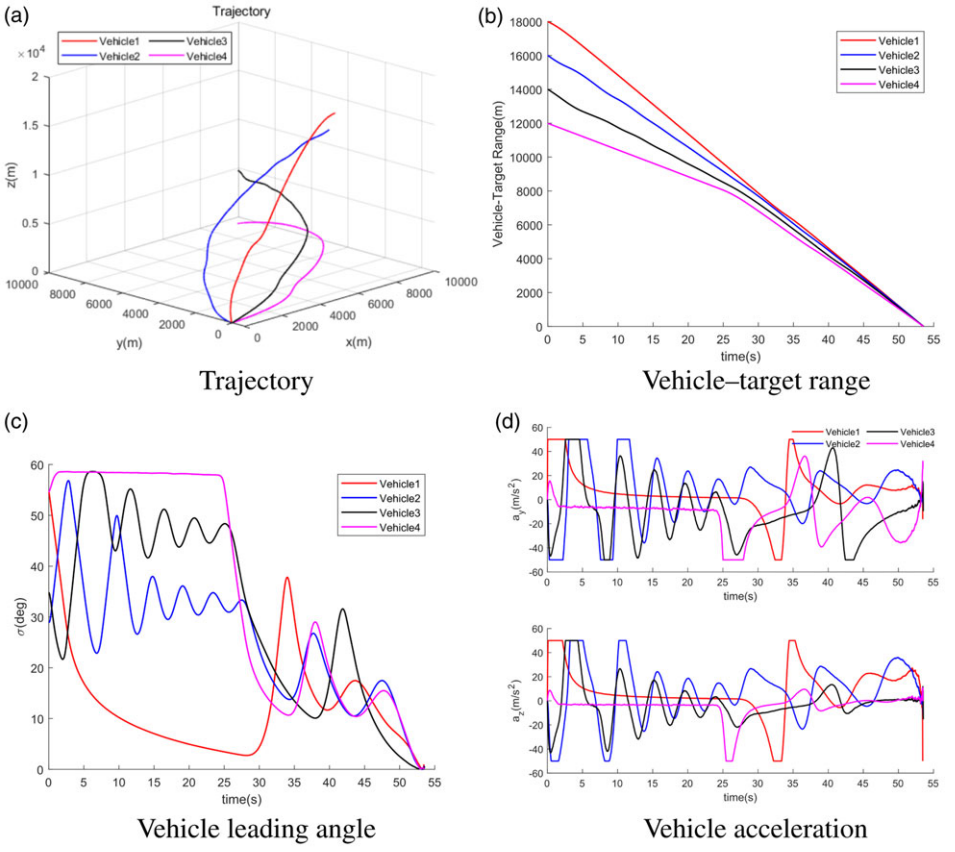


Figure 11. *Guidance results with communication delay and measurement noise.*

$$A = \begin{bmatrix} 0 & 1 & 0 & 1 \\ 1 & 0 & 1 & 0 \\ 0 & 1 & 0 & 1 \\ 1 & 0 & 1 & 0 \end{bmatrix}. \tag{59}$$

Figure 8 shows the simulation results from the proposed guidance law. It can be seen that the proposed guidance law works effectively, and the FOV constraints are never violated.

In order to illustrate the robustness of the proposed guidance law, we implemented simulations for the following scenarios: (1) verification of effectiveness under different communication network topologies; (2) the case where the initial conditions do not satisfy the constraints; and (3) the presence of communication delays and measurement noise.

A communication network topology similar to the leader-follower structure was considered, with the corresponding adjacent matrix presented below. The simulation results are shown in Fig. 9. It can be observed that the performance of the proposed guidance law is not sensitive to the communication network topology.

$$A = \begin{bmatrix} 0 & 1 & 0 & 0 \\ 1 & 0 & 1 & 1 \\ 0 & 1 & 0 & 0 \\ 0 & 1 & 0 & 0 \end{bmatrix} \tag{60}$$

https://doi.org/10.1017/aer.2024.129 Published online by Cambridge University Press

To demonstrate the robustness of the proposed guidance law in the face of extreme scenarios, we consider a scenario in which the initial condition of a number of vehicles do not satisfy the FOV constraints, where $\sigma_1\ (t_0) = 65, \sigma_2\ (t_0) = 71, \sigma_4\ (t_0) = 67$, the values are expressed in degrees. The simulation results are shown in Fig. 10. It can be seen that despite the initial conditions not satisfying the requirements of Lemma 1, the proposed guidance law still works and the FOV angle of the vehicle rapidly converging on the constraint region and being maintained until arrived at the target.

To illustrate the robustness of the proposed guidance law in a more realistic setting, we conduct simulations with measurement noise and communication delays. In this case, the measurement noises are added to $r_i, v_i, \theta_{Li}, \psi_{Li}, \theta_{mi}, \psi_{mi}$, and the signal-to-noise ratio is set to 50dB. Furthermore, information transmissions between vehicle have a time delay of 0.5 seconds. As shown in Fig. 11, the proposed guiding law has a stable performance despite measurement noise and communication delays.

5.0 Conclusion

A distributed cooperative guidance law considering FOV constraints without numerical singularities is proposed. The proposed guidance law has the following advantages: (1) the FOV constraint of vehicles is taken into account in the design of the guidance law; (2) it has no numerical singularities and does not require accurate time-to-flight estimates; (3) the proposed guidance law is distributed, which means that the vehicles do not need the global information from all the vehicles. Through numerical simulation and comparative study, the effectiveness and robustness of the proposed guidance law are validated.

The next research work can be considered from the following aspects: (1) modifying the proposed guidance law so that it can be suitable for manoeuvering target; (2) design and stability analysis of cooperative guidance law in the case of switched communication topology or time-varying communication topology; (3) event-triggered technology can be introduced into the design of guidance law to reduce the resource utilisation burden between vehicles.

Competing interests. The authors declare none.

References

[1] Liu, S., Wang, Y., Li, Y., Yan, B. and Zhang, T. Cooperative guidance for active defence based on line-of-sight constraint under a low-speed ratio, *Aeronaut. J.*, 2023, **127,** (1309), pp 491–509.
[2] Chen, Y., Wang, J., Wang, C., Shan, J. and Xin, M. A modified cooperative proportional navigation guidance law, *J. Frank. Inst.*, 2019, **356,** (11), pp 5692–5705.
[3] Jeon, I.-S, Lee, J.-I. and Tahk, M.-J. Impact-time-control guidance law for anti-ship missiles, *IEEE Trans. Control Syst. Technol.*, 2006, **14,** (2), pp 260–266.
[4] Liu, S., Yan, B., Liu, R., Dai, P., Yan, J. and Xin, G. Cooperative guidance law for intercepting a hypersonic target with impact angle constraint, *Aeronaut. J.*, 2022, **126,** (1300), pp 1026–1044.
[5] Shiyu, Z., Rui, Z., Chen, W. and Quanxin, D. Design of time-constrained guidance laws via virtual leader approach, *Chin. J. Aeronaut.*, 2010, **23,** (1), pp 103–108.
[6] Saleem, A. and Ratnoo, A. Lyapunov-based guidance law for impact time control and simultaneous arrival, *J. Guid. Control Dyn.*, 2016, **39,** (1), pp 1–9.
[7] Lee, J.-I., Jeon, I.-S. and Tahk, M.-J. Guidance law to control impact time and angle, *IEEE Trans. Aerospace Electron. Syst.*, 2007, **43,** (1), pp 301–310.
[8] Kim, Y.-C., Lee, C.-H., Kim, T.-H. and Tahk, M.-J. A new cooperative homing guidance of anti-ship missiles for survivability enhancement, *Int. J. Aeronaut. Space Sci.*, 2021, **22**, pp 676–686.
[9] Kang, S., Wang, J., Li, G., Shan, J. and Petersen, R.I. Optimal cooperative guidance law for salvo attack: An mpc-based consensus perspective, *IEEE Trans. Aerospace Electron. Syst.*, 2018, **54,** (5), pp 2397–2410.
[10] Pei, H. Group consensus of multi-agent systems with hybrid characteristics and directed topological networks, ISA Trans., 2023, **404**, pp 267–275.
[11] He, L. and Dong, W. Distributed adaptive consensus tracking control for heterogeneous nonlinear multi-agent systems, *ISA Trans.*, 2022, **130**, pp 177–183.
[12] Lu, M., Wu, J., Zhan, X., Han, T. and Yan, H. Consensus of second-order heterogeneous multi-agent systems with and without input saturation, *ISA Trans.*, 2022, **126**, pp 14–20.
[13] Meng, W., Yang, Q., Si, J. and Sun, Y. Consensus control of nonlinear multiagent systems with time-varying state constraints, *IEEE Trans. Cybern.*, 2017, **47,** (8), pp 2110–2120.

https://doi.org/10.1017/aer.2024.129 Published online by Cambridge University Press

[14] Fu, J., Wen, G., Yu, W., Huang, T. and Yu, X. Consensus of second-order multiagent systems with both velocity and input constraints, *IEEE Trans. Ind. Electron.*, 2019, **66,** (10), pp 7946–7955.
[15] Wang, Z., Fu, W., Fang, Y., Zhu, S., Wu, Z. and Wang, M. Prescribed-time cooperative guidance law against maneuvering target based on leader-following strategy, *ISA Trans.*, 2022, **129**, pp 257–270.
[16] Zhou, J. and Yang, J. Distributed guidance law design for cooperative simultaneous attacks with multiple missiles, *J. Guid. Control Dyn.*, 2016, **39**, pp 2439–2447.
[17] Sinha, A., Ranjan Kumar, S. and Mukherjee, D. Three-dimensional nonlinear cooperative salvo using event-triggered strategy, J. Guid. Control Dyn., 2021, **44**, (2), pp 328–342.
[18] Li, K., Wang, J., Lee, C.-H., Zhou, R. and Zhao, S. Distributed cooperative guidance for multivehicle simultaneous arrival without numerical singularities, *J. Guid. Control Dyn.*, 2020, **43**, (7), pp 1365–1373.
[19] Chen, Y., Wang, J., Wang, C., Shan, J. and Xin, M. Three-dimensional cooperative homing guidance law with field-of-view constraint, *J. Guid. Control Dyn.*, 2020, **43,** (2), pp 389–397.
[20] Wang, X. and Lu, X. Three-dimensional impact angle constrained distributed guidance law design for cooperative attacks, *ISA Trans.*, 2018, **73**, pp 79–90.
[21] Ma, W., Fu, W., Fang, Y., Liu, S. and Liang, X. Prescribed-time cooperative guidance with time delay, *Aeronaut. J.*, 2023, **127,** (1311), pp 852–875.
[22] Yang, G., Fang, Y., Ma, W., Zhu, S. and Fu, W. Cooperative trajectory shaping guidance law for multiple anti-ship missiles, *Aeronaut. J.*, 2024, **128,** (1319), pp 73–91.
[23] Wu, G., Zhang, K. and Han, Z. Three-dimensional finite-time guidance law based on sliding mode adaptive rbf neural network against a highly manoeuvering target, *Aeronaut. J.*, 2022, **126,** (1301), pp 1124–1143.
[24] He, S. and Lee, C.-H. Optimal proportional-integral guidance with reduced sensitivity to target maneuvers, *IEEE Trans. Aerospace Electron. Syst.*, 2018, **54**, (5), pp 2568–2579.
[25] Jesus, A.T., Pimenta, C.A.L., Tôrres, A.B.L. and Mendes, M.A.M.E. Consensus for double-integrator dynamics with velocity constraints, *Int. J. Control Autom. Syst.*, 2014, **12**, pp 930–938.
[26] Song, S.-H. and Ha, I.-J. A lyapunov-like approach to performance analysis of 3-dimensional pure png laws, *IEEE Trans. Aerospace Electron. Syst.*, 1994, **30**, (1), pp 238–248.

Cite this article: Liu Z., Li S., Ren L. and Ma D. (2025). Distributed cooperative guidance law without numerical singularity with field-of-view angle constraint. *The Aeronautical Journal*, **129**, 1515–1533. https://doi.org/10.1017/aer.2024.129

https://doi.org/10.1017/aer.2024.129 Published online by Cambridge University Press